

© The Authors 2023. Open access.
Content is available under Creative Commons Attribution
License 4.0 International (CC BY 4.0)



© Авторы 2023 г. Открытый доступ.
Контент доступен по лицензии Creative Commons Attribution
License 4.0 International (CC BY 4.0)

УДК 550.344.42

<https://doi.org/10.30730/gtr.2023.7.3.292-303>

<https://www.elibrary.ru/rcsgya>

Data selection method for restoring a tsunami source form

Tatyana A. Voronina^{@1}, Vladislav V. Voronin²

@ E-mail: tanvor@bk.ru

¹Institute of Computational Mathematics and Mathematical Geophysics, SB RAS, Novosibirsk, Russia

²Novosibirsk State University, Novosibirsk, Russia

Abstract. The reconstruction of a tsunami source as a solution to the inverse problem in mathematical physics relies on the use of the truncated singular value decomposition method (a variant of the least squares method) for inverting remote records of the tsunami wave. The proposed method allows one to overcome the inevitable instability of the numerical solution. The result of inversion depends on the choice of the observation system, actual bathymetry and data noise level. Within the developed approach, a methodology for choosing key inversion options and an optimal dataset which provide the best accuracy of a tsunami source recovery is discussed. It is based on analyzing the distribution of the specific energy generated by all spatial modes at the locations of the active sensors. The peculiarity of the algorithm is that the use of the most informative data allows one without re-computation of the direct problem to obtain wave amplitudes at the points of interest (let us call them as “fictitious” stations) where there were no observations, but those that were considered in preliminary calculations. Three real-life events, the Chilean Illapel tsunami on September 16, 2015, the tsunami near the Solomon Islands on February 6, 2013, and the Shikotan tsunami on October 5, 1994, are used as examples of the proposed approach. The results obtained allow one hope for using of this approach in practice.

Keywords: inverse ill-posed problem, singular value decomposition, specific energy, numerical modeling

Метод выбора данных для восстановления формы источника цунами

Т. А. Воронина^{@1}, В. В. Воронин²

@ E-mail: tanvor@bk.ru

¹Институт вычислительной математики и математической геофизики СО РАН, Новосибирск, Россия

²Новосибирский государственный университет, Новосибирск, Россия

Резюме. Восстановление исходной формы источника цунами как решение обратной задачи математической физики основано на использовании метода усеченного сингулярного разложения (вариант метода наименьших квадратов) для обращения удаленных записей волны цунами. Предложенный метод позволяет преодолеть неизбежную нестабильность численного решения. Результат инверсии зависит от выбора системы наблюдения, фактической батиметрии и уровня шума данных. В рамках разработанного подхода обсуждается методика выбора ключевых параметров инверсии и оптимального набора данных, обеспечивающих максимальную точность восстановления формы источника цунами. Метод основан на анализе распределения удельной энергии, генерируемой всеми пространственными модами в местах расположения действующих датчиков. Особенность алгоритма состоит в том, что использование наиболее информативных данных позволяет без повторных расчетов прямой задачи получить амплитуды волн в интересующих точках (назовем их «фиктивными» станциями), где не было наблюдений, но которые были учтены в предварительных расчетах. В качестве примеров применения предлагаемого подхода использованы три реальных события: чилийское цунами Иллапель 16 сентября 2015 г., цунами у Соломоновых островов 6 февраля 2013 г. и Шикотанское цунами 5 октября 1994 г. Полученные результаты позволяют надеяться на применение данного подхода на практике.

Ключевые слова: обратная некорректная задача, сингулярное разложение, удельная энергия, численное моделирование

Funding and Acknowledgements

The research was supported by the State Budget Program for the Institute of Computational Mathematics and Mathematical Geophysics of SB RAS (no. 0315-2023-0005).

Authors are grateful to the respected Reviewers for their constructive comments and recommendations.

For citation: Voronina T.A., Voronin V.V. Data selection method for restoring a tsunami source form. *Geosistemy perekhodnykh zon = Geosystems of Transition Zones*, 2023, vol. 7, no. 3, pp. 292–303. (In Engl., abstr. in Russ.). <https://doi.org/10.30730/gtr.2023.7.3.292-303>; <https://www.elibrary.ru/rcsgya>

Introduction

Numerous tsunami observation networks are currently deployed in large tsunami-prone regions, providing a wealth of data for real-time tsunami monitoring. The effectiveness of tsunami warning is an important factor in choosing locations for measuring instruments [1]. In particular, sensor placement for tsunami observation is often associated with historical records in the area of interest, usually confirmed by expert judgments on various decisive factors including technical and financial constraints [2]. Processing of a large amount of data required the use of optimization methods for the number of observations and the optimal time of tsunami warning [3, 4]. Conclusions about the effectiveness of the sensor system are usually based on the analysis of an exhaustive number of synthetic experiments with hypothetical tsunami scenarios, such as in [5].

This paper describes a technique for selecting the optimal data set and inversion parameters. The locations of the most informative sensors are determined based on analyzing the distribution of the specific energy by all spatial modes at the locations of the sensors (the specific energy is an energy per unit volume of fluid). The physics of the deep focus is not considered in this study that is aimed at restoring an initial tsunami waveform when data processing.

The proposed approach is based on our studies of using the truncated singular value decomposition method (a variant of the least squares method) for determining the initial tsunami waveform (often replaced by the tsunami source) by inverting remote records of the transmitted wave [6–8].

Финансирование и благодарности

Исследования выполнены в рамках государственного задания Института вычислительной математики и математической геофизики СО РАН (№ 0315-2023-0005).

Авторы признательны рецензентам за конструктивные замечания и рекомендации.

As our studies have shown, an increase in the total number of observed records, due to their significant noise level, fails to increase the inversion accuracy for the considered ill-posed problem [8]. On the contrary, by excluding noninformative records we can increase significantly the reliability of source function recovery.

The important feature of developed algorithm is as follows: by using the most informative data, there is no need to re-solve the direct problem with recovered tsunami source. Within solving the direct problem, the theoretical marigrams from model sources should be calculated not only at the locations of the actual sensors, but also at points of interest. We named these points as the “fictitious” stations.

The proposed approach has been tested against three actual events: the Chilean Illapel tsunami on September 16, 2015, the tsunami near the Solomon Islands on February 6, 2013 and the Shikotan tsunami on October 5, 1994. The events in question were triggered by earthquakes with a magnitude of 8.0–8.3, but had significant differences in bathymetry on the path of tsunami waves from the source area to monitoring stations.

The method

A detailed description of the mathematical formulation is presented in [6]. The problem of determining a tsunami source by the known records of a tsunami in a set of remote points is posed as an ill-posed inverse problem of mathematical physics. It is assumed that the tsunami source is a vertical displacement of the ocean floor caused by the main shock of the earthquake

(the piston model of tsunami). The free surface level function $\eta(x, y, t)$ can be found as the solution of the linearized “shallow water” equations with total reflecting boundary conditions on the coast and absorbing boundary conditions on an open sea boundary:

$$\eta_{tt} = \nabla^T (gh(x, y) \nabla \eta) \quad (1)$$

$$\eta|_{t=0} = \varphi(x, y); \quad \eta_t|_{t=0} = 0; \quad (2)$$

$$\frac{\partial \eta}{\partial \mathbf{n}}|_S = 0; \quad -c\mathbf{V} \cdot \mathbf{n} - \eta_{tt} + \frac{c^2 \partial^2 \eta}{2\partial \tau^2}|_\Gamma = 0, \quad (3)$$

where \mathbf{n} is the external normal vector to the solid wall, τ is a tangent direction at the boundary, $h(x, y)$ is the smooth function describing the bottom topography, g is the acceleration of gravity, $\mathbf{V} = (\eta_{xt}, \eta_{yt})$ the phase velocity of the wave is defined as $c(x, y) = \sqrt{gh(x, y)}$. The condition of an absolutely reflective solid wall is satisfied on the coastline S . On the so-called open sea boundaries Γ , this algorithm implements the absorbing boundary conditions of the second order of accuracy. The mathematical formulation of the problem under these assumptions consists in determining the initial displacement of the free surface $\eta(x, y, t)|_{t=0} = \varphi(x, y)$ in the area of the tsunami source (the target domain) the rectangle $\Omega = [l_1 \times l_2]$, wherein the values of l_1, l_2 are assumed to be known from the seismic information. The proposed method requires only approximate information about the location of the tsunami source. It is also assumed that oscillations in the level of the free sea surface are known at a certain set of points

$$M = \{(x_i, y_i), i = 1, \dots, P\}; \quad \eta(x, y, t)|_M = \eta_0(x_i, y_i, t).$$

Modeling of direct problem is carried out using a finite-difference approach. Aimed to solve the inverse problem, the unknown function is searched in the form of a finite segment of the Fourier series in spatial harmonics with unknown coefficients $\{c_{mn}\}$:

$$\begin{aligned} \varphi(x, y) &= \sum_{m=1}^M \sum_{n=1}^N c_{mn} \sin \frac{m\pi}{l_1} x \sin \frac{n\pi}{l_2} y = \\ &= \sum_{m=1}^M \sum_{n=1}^N c_{mn} \varphi_{mn}(x, y) \end{aligned} \quad (4)$$

A similar methodology is employed, e.g., in NOAA [9], where the initial tsunami waveform is

determined via the least residual method applied to a set of known base models.

The problem under consideration is ill-posed, the numerical solution is unstable and, hence, a regularization procedure is required. To this end, the least squares inversion using a truncated singular value decomposition (SVD) method (hereinafter, the r -solution method) was applied. In other words, the regularization of the operator is carried out by restricting the operator to a subspace that is a linear span of the first right singular vectors.

To find the coefficients $\{c_{mn}\}$ a linear system (the “key” system) is constructed:

$$\mathbf{A} \vec{c} = \vec{\eta}_0, \quad (5)$$

where the vector $\vec{c} = \{c_{mn}\}$. To obtain the columns of matrix \mathbf{A} , one should numerically solve the direct problem (1)–(3), when every harmonic $\varphi_{mn}(x, y)$ from the sum (4) is used as an initial displacement. In this way, \mathbf{A} is a matrix whose columns consist of the waveforms have been computed at the locations of all active sensors. If one intends to predict the marigrams at points of interest, the marigrams for each harmonic should in addition be calculated at those points, too. Using the notation $\eta_{pj} = \eta(x_p, y_p, t_j)$, one can write the vector $\vec{\eta}_0$ consisting of the observed marigrams in the form: $\vec{\eta}_0 = (\eta_{11}, \eta_{12}, \dots, \eta_{1N_t}, \eta_{21}, \dots, \eta_{2N_t}, \dots, \eta_{P1}, \dots, \eta_{PN_t})$, where $(x_p, y_p), p = 1, \dots, P$ are the finite number of active sensors. The free surface oscillations are assumed to be known for a finite number of times $\{t_j\}, j = 1, \dots, N_t$ in every sensor.

It should be noted that the calculation of the matrix \mathbf{A} is the most time-consuming part of the algorithm.

Next, SVD decomposition is computed for the matrix \mathbf{A} and a generalized normal r -solution of the system (5) approximating the initial tsunami waveform is constructed:

$$\begin{aligned} \varphi^{[r]}(x, y) &= \sum_{j=1}^r \alpha_j \vec{v}_j(x, y) = \\ &= \sum_{j=1}^r \alpha_j \sum_{m=1}^M \sum_{n=1}^N \beta_{mn}^j \varphi_{mn}(x, y) \end{aligned} \quad (6)$$

Here $\alpha_j = \frac{(\vec{\eta}_0 \cdot \vec{u}_j)}{s_i}$, $\{s_i, \vec{u}_i, \vec{v}_i\}$ are singular numbers, right and left singular vectors of the matrix \mathbf{A} . The ill-posedness of the problem manifests itself in the rapid decay of the singular values which is limiting the key parameter r of the r -solution (6).

Selecting inversion options

By varying the value of r in formula (6), one can control the instability of the numerical solution. Naturally, with an increase in the value of r , the information content of the resulting r -solution increases, but the numerical stability deteriorates. It is clear that the number r is a key parameter regarding the reliability of the inversion. The value of r is determined by the behavior of the singular spectrum, which in turn depends on the observation system, bathymetry, and the level of noise in the data. Based on numerical experiments with three real-life events, we are going to illustrate

three ways to choose the value of r . First, introduce the notations:

Model 1. Illapel Tsunami on September 16, 2015, observation system: DART buoys (1-2402, 2-32401, 3-32412, 4-32411, 5-43413), $P = 5$; $N_t = 1001$; $\Delta t = 4$ sec; the simulation domain – $102^\circ \text{ W} \leq x \leq 70^\circ \text{ W}$; $12^\circ \text{ N} \leq y \leq 38^\circ \text{ S}$ is shown in Fig. 1 a.

Model 2. Tsunami near the Solomon Islands on February 06, 2013, observation system: DART buoys (1-55012, 2-55023, 3-52403, 4-52402, 5-52406, 6-51425), $P = 6$; $N_t = 1201$; $\Delta t = 4$ sec; the simulation domain – $140^\circ \text{ E} \leq x \leq 185^\circ \text{ E}$, $13^\circ \text{ N} \leq y \leq 17^\circ \text{ S}$ is shown in Fig. 1 b.

Model 3. Shikotan Tsunami on 05.10.1994, observation system, as in [10], the locations of these coastal tide gauges are shown in Fig. 1 c: 1 – Kushiro, 2 – Tokachikou, 3 – Hakodate (Hokkaido Island), as well as 4 – Hachinohe and 5 – Miyako (Honshu Island), $P = 5$; $N_t = 162$ min;

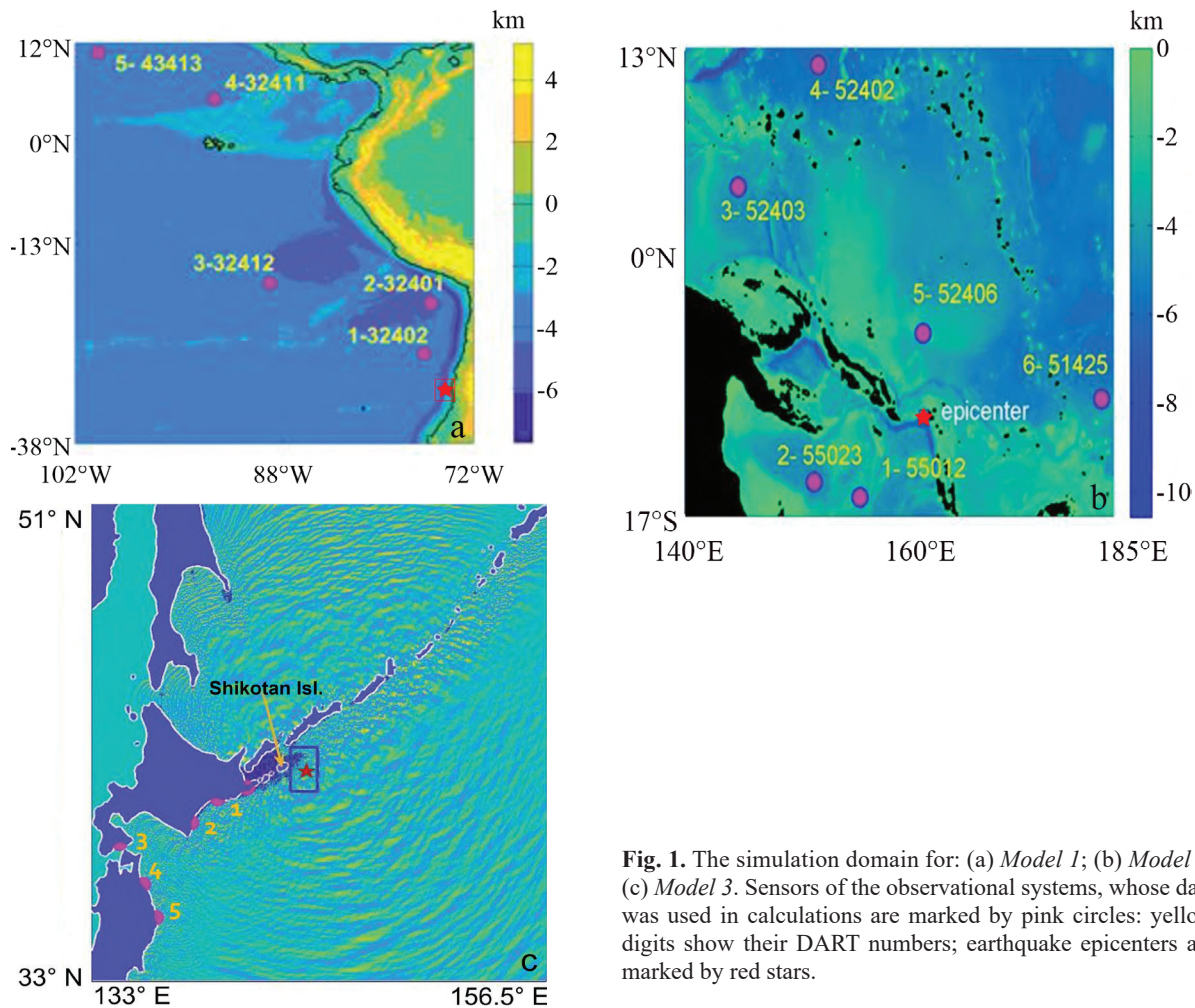


Fig. 1. The simulation domain for: (a) *Model 1*; (b) *Model 2*; (c) *Model 3*. Sensors of the observational systems, whose data was used in calculations are marked by pink circles: yellow digits show their DART numbers; earthquake epicenters are marked by red stars.

the simulation domain: $133^{\circ} E \leq x \leq 156.5^{\circ} E$; $33^{\circ} N \leq y \leq 51^{\circ} N$. The bathymetry used is based on the GEBCO data <http://www.gebco.net>. The data of the Shikotan tsunami are not deep-sea one, also, this data was not synchronized. The locations of the above tide gauges and bathymetry of the western slope of the Kuril-Kamchatka Trench gave a reason to add this event to our study as an experiment. Is it possible to evaluate the information significance of these sensors using proposed approach?

First numerical experiments with model sources, aimed at choosing the “best” observation system, were based solely on the analysis of singular spectra of matrix **A** for different observation systems [8]. The longer the first flat section of the spectrum graph, the larger value of r can be used. Comparing the plots in Fig. 2 a, one can expect that the reconstruction of the tsunami source using the set of sensors {4, 5, 6} will be less successful,

since the nature of the spectrum of the corresponding matrix (the magenta line) allows one to use a significantly lower value of r . This assumption is confirmed within further computations.

It has been found that a smaller set of sensors can provide a more “attractive” spectrum. However, this method turned out to be significantly time-consuming, as it requires iterating over a large number of versions of the observation system. In addition, the choice of the best observation system is complicated if the lines of the spectra are sufficiently similar.

To reduce the search time for an optimal value of r , the following method was proposed in [11]. It is known that the right and left singular vectors form the bases in the solution space and data space, respectively. The components of each right-singular vector $\{\beta_{mn}\}$ are the coefficients at the spatial harmonics in the source function. As-

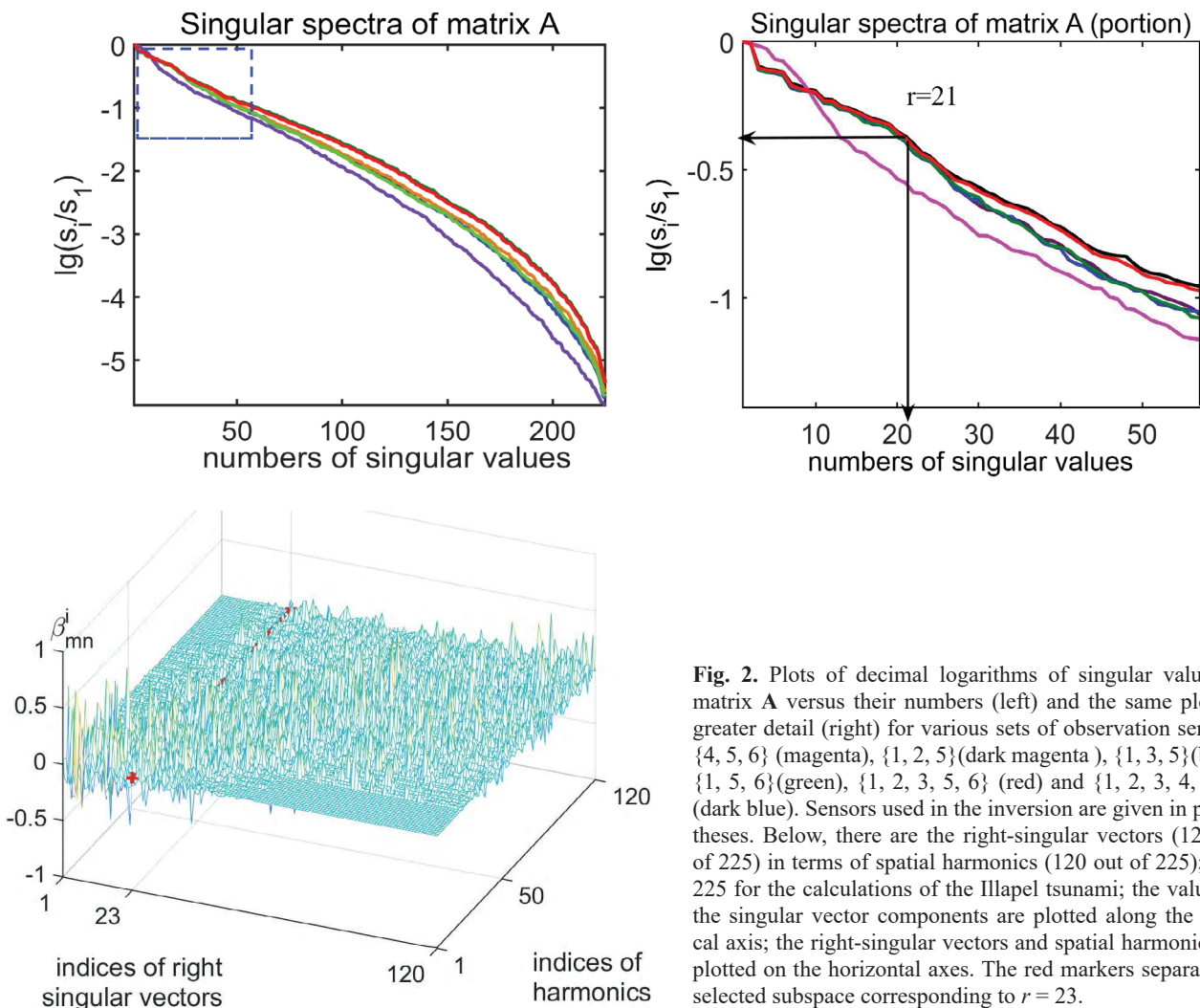


Fig. 2. Plots of decimal logarithms of singular values of matrix **A** versus their numbers (left) and the same plots in greater detail (right) for various sets of observation sensors: {4, 5, 6} (magenta), {1, 2, 5} (dark magenta), {1, 3, 5} (blue), {1, 5, 6} (green), {1, 2, 3, 5, 6} (red) and {1, 2, 3, 4, 5, 6} (dark blue). Sensors used in the inversion are given in parentheses. Below, there are the right-singular vectors (120 out of 225) in terms of spatial harmonics (120 out of 225); total 225 for the calculations of the Illapel tsunami; the values of the singular vector components are plotted along the vertical axis; the right-singular vectors and spatial harmonics are plotted on the horizontal axes. The red markers separate the selected subspace corresponding to $r = 23$.

sume the harmonics are numbered in ascending order of $\gamma_{mn} = (m/l_1)^2 + (n/l_2)^2$ (“oscillation index”), where m and n are indices of spatial harmonics l_1, l_2 are sizes of the target domain in longitude and latitude directions, respectively. The large values of the oscillation index correspond to the high-frequency harmonics, causing the appearance of non-physical artifacts in the solution. To avoid this problem, one should use only those right singular vectors in which the high-frequency components corresponding to large γ_{mn} are sufficiently small. Selection of solution subspace by this method for *Model 1* is presented in Fig. 2 b: the red line with the red marker separates those right-singular vectors, whose coefficients at high-frequency harmonics are weakly manifested (here we follow the concept of [11]). To suppress high-frequency components in the solution, one can, for example, set a limit to $r = 23$. For greater accuracy,

one will have to use several values of r . Note that the complete absence of high-frequency components will lead to a loss of amplitude accuracy.

In the course of numerical experiments with model sources ([8]) it turned out that the location of the tsunami monitoring stations in the directions of the “greatest variability” of the source has a significant effect on the quality of inversion. Our subsequent studies with the real-life events shown that the revealed direction coincide with the direction of the most intensive propagation of wave energy. That’s why, a more promising approach seemed to us to analyze the location of the sensors in terms of the accumulation of specific energy. The specific energy is an energy per unit volume of fluid.

The similar approach was employed in [4] for the purpose to infer the parameters of hypothetical tsunami sources, in terms of the fault slip distribution around the Nankai Trough, Japan.

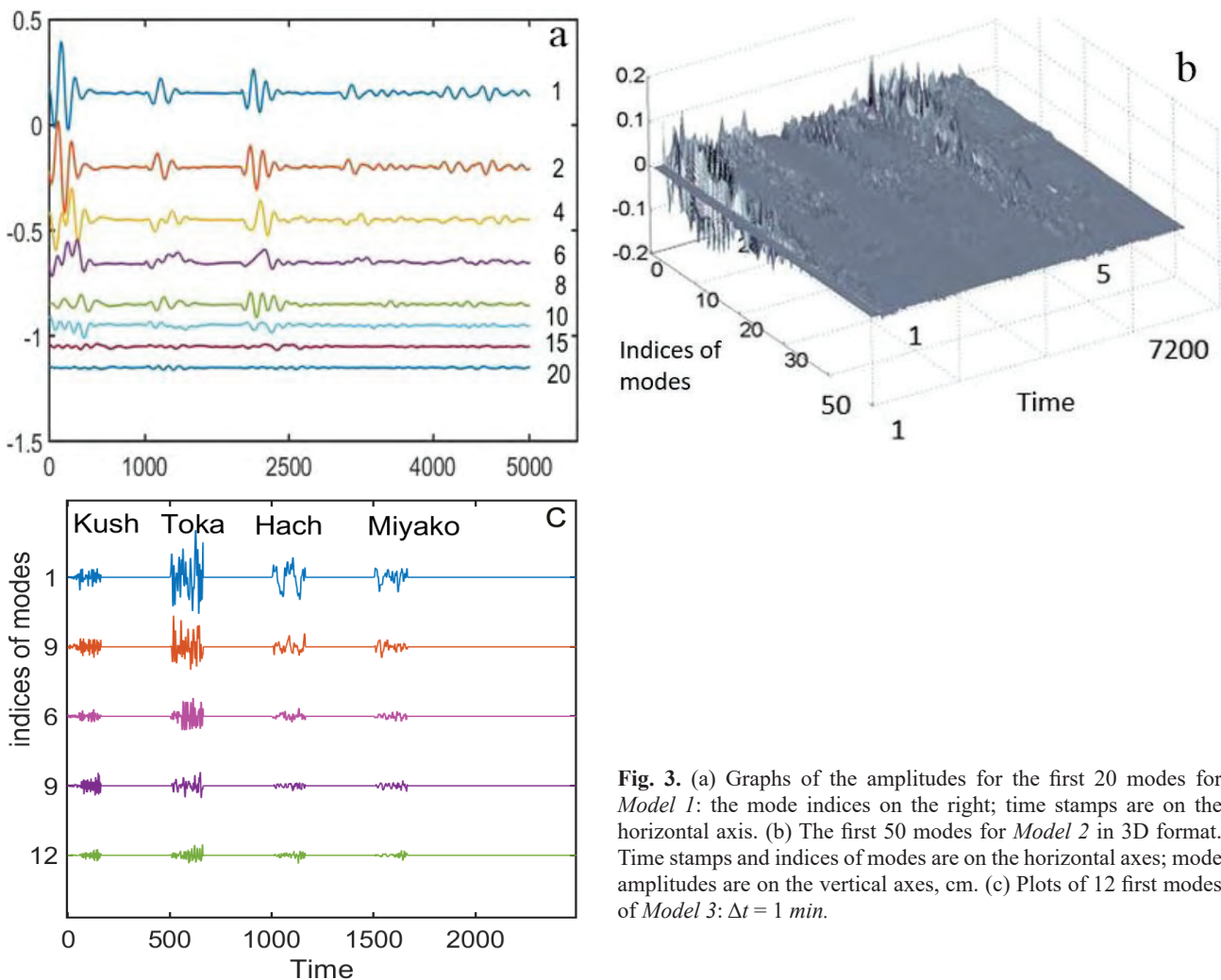


Fig. 3. (a) Graphs of the amplitudes for the first 20 modes for *Model 1*: the mode indices on the right; time stamps are on the horizontal axis. (b) The first 50 modes for *Model 2* in 3D format. Time stamps and indices of modes are on the horizontal axes; mode amplitudes are on the vertical axes, cm. (c) Plots of 12 first modes of *Model 3*: $\Delta t = 1 \text{ min}$.

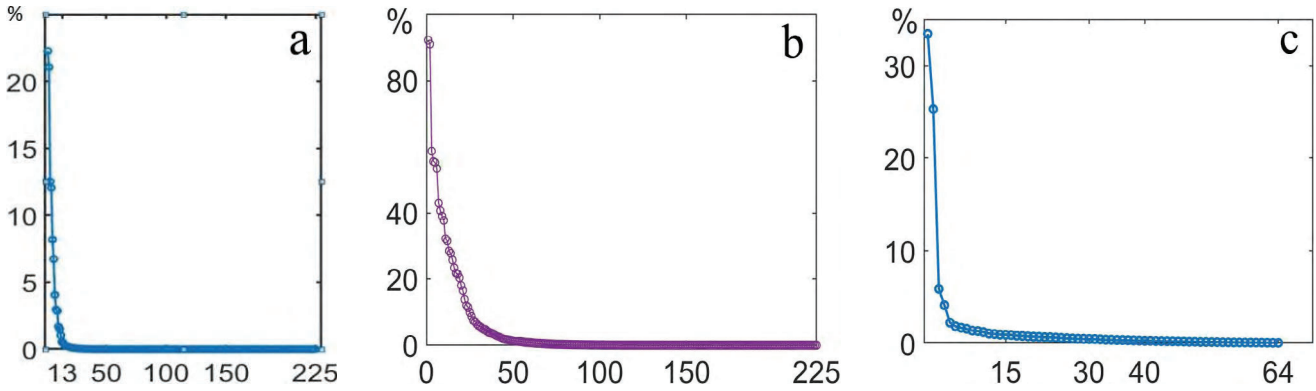


Fig. 4. Distribution of the specific energy vs. spatial mode indices: (a) *Model 1*; (b) *Model 2*; (c) *Model 3*. On the horizontal axes: the mode indices; on the vertical axes: the percentage of specific energy carried by each mode.

In this paper, we discuss a technique for using the distribution of the specific energy between the sensors of the observation system to select the number r . Each right singular vector $\bar{\mathbf{v}}_i$ generates the space $\mathbf{s}_i \bar{\mathbf{u}}_i$ mode according to the SVD formula $\mathbf{A} \bar{\mathbf{v}}_i = \mathbf{s}_i \bar{\mathbf{u}}_i$, $i = 1, M \times N$. The specific energy per mass unit of fluid is proportional to the sum of the squared deviations of the time series (for observed marigrams or for each mode). Considering the sharp decrease in singular values, it can be argued that only the first spatial modes (corresponding to the first singular values) are significant in terms of information (energy) transfer. Decreasing in modes amplitudes with increasing their numbers in the models under consideration is well confirmed in Fig. 3. Namely, the amplitude plots of the first 20 modes for *Model 1* are shown in Fig. 3 a. The first 50 modes for *Model 2* in 3D format are represented in Fig. 3 b. In Fig. 3 c there are 12 spatial modes computed for *Model 3* (note: the 3-Hakodate tide gauge was excluded from the observation system due to insufficient data). The lengths of modes (time-counts with 4 sec intervals) are equal to $5005 = 1001 \times 5$; $7200 = 1200 \times 6$ for the Model 1, 2, and $2000 = 500 \times 4$ (time-counts with 1 min intervals), for the Model 3, respectively.

Another method to determine an upper bound on r is based on analyzing the distribution of the specific energy over all modes. More precisely, the upper limit can be set by determining the number of spatial modes that carry a significant share of the total specific energy. The share of specific energy i -th mode can be characterized

as $s_i^2 / \sum_i s_i^2$. In Fig. 4 the share of specific energy is shown as a function of the mode index i for the considered real-life events. Figure 4 a: *Model 1*, the graph of the distribution of the specific energy over modes. The first 15 modes associated with the maximum singular values carry 80 % of the energy, i.e. $r \leq 15$. Figure 4 b shows the dependence for *Model 2*. The total number of modes is equal to 225. The total shares of the first 21 modes accumulate more than 83 % of the total specific energy, the first 25 modes: more than 88 %. Therefore, this method limits the value of r as $r \leq 25$. For *Model 3*, the total shares of the first 16 modes accumulate more than 90 % of the total specific

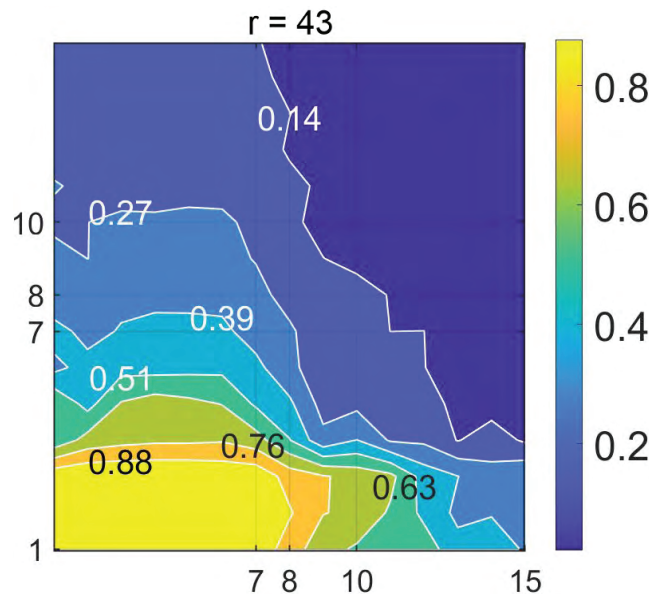


Fig. 5. *Model 1*. The level lines of the projections of the harmonics onto the solution subspace when $r = 43$ and $N = 15$, $M = 15$; indices n is on the horizontal axis; indices m is on the vertical axis.

energy, see Fig. 4 c. This limits the value of $r \leq 16$ when the total number of modes is equal to 64.

Thus, by applying the SVD procedure and analyzing the distribution of the specific energy over modes (in terms of singular values), one can choose a reasonable value of the parameter r for the inversion. After that, one can determine the number of spatial harmonics to be used in the source approximation. As it has been shown in [11], the recovery of high-frequency harmonics strongly depends on the subspace dimension. The smaller r , the more harmonics are not restored and get replaced by numerous “parasitic” harmonics, which leads to the appearance of the artifacts in the solution. To determine the values of M and N , we set a threshold for the projection length of the harmonics onto the solution subspace under consideration. The projection length is calculated as the cosine of the angle of the spatial harmonic with the selected subspace. For example, the isolines of these projections onto the subspace with $r = 3$ are shown in Fig. 5 for *Model 1*.

As was established experimentally, the threshold value of the cosine must be at least 0.5, smaller values indicate a weak representation of such harmonic on the selected subspace, i.e., in the solution. On the contrary, an increase in this value leads to a loss of extreme values of the amplitudes. For example, it is clear from Fig. 5 that using harmonics with indices $m \geq 4$ and with indices $n \geq 10$ will lead to the appearance of numerous artifacts in the solution.

Selection of the most “informative” observational data

Based on numerical experiments, we have concluded that a reliable reconstruction of the tsunami source can be reached when the used observation stations supply at least 2/3 of the total specific energy.

Модель 1. The diagram in Fig. 6 a shows that data of the DART buoys 1-32402 and 2-32401 accumulated 71.19 % of the total specific wave

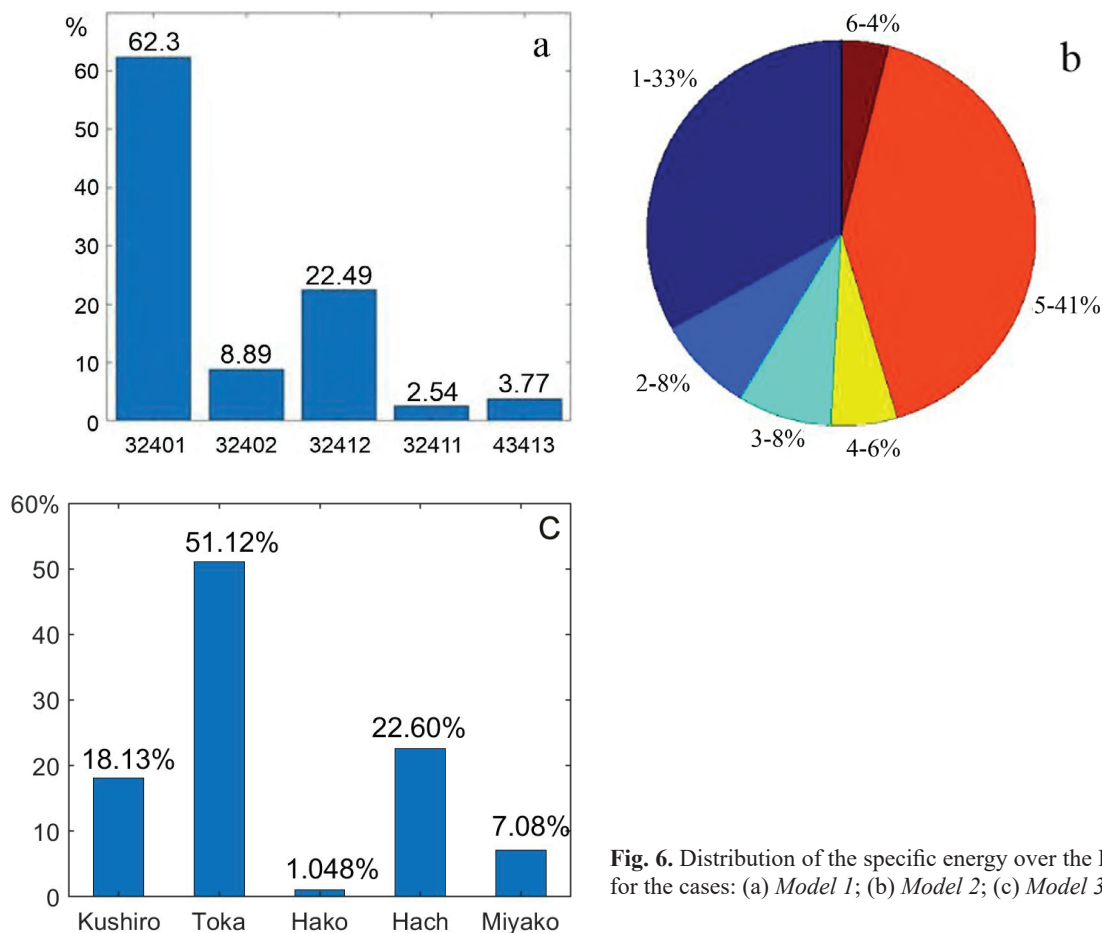


Fig. 6. Distribution of the specific energy over the DART buoys for the cases: (a) *Model 1*; (b) *Model 2*; (c) *Model 3*.

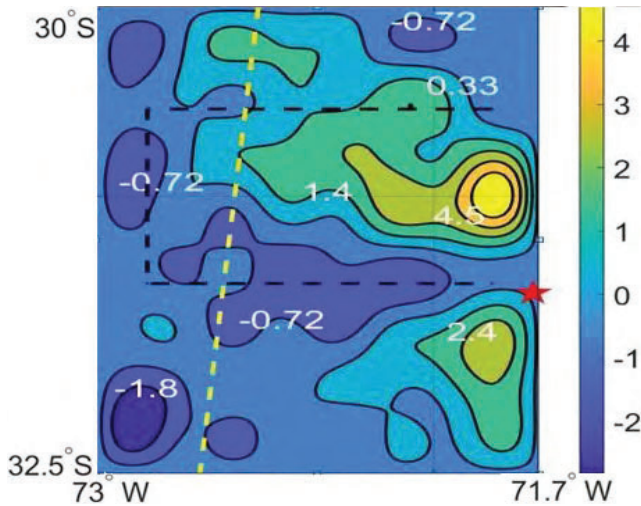


Fig. 7. Model 1. The initial sea-surface displacements as inversion result based on the data recorded by DART buoys 1-32402 and 2-32401. Displacement of the sea surface scaled in *m*. On the horizontal and on the vertical axes: there are the longitude and the latitude directions (in degrees), respectively; the yellow dotted line is marking the axis of the Atakama Trench; the epicenter of the earthquake is marked the red star.

energy recorded in the entire observation system. The record of the DART buoy 3-32412 has not been used because it has been corrupted. Data of DART buoys 1-32402 and 2-32401 were defined as the most “informative”. The inversion based on these data allows one to restore the tsunami source with a sufficient accuracy (Fig. 7) that provides a good agreement with the results obtained by other researchers [13].

Moreover, in the above case the wave amplitudes in the locations of the DART buoys 4–32411 and 5-43413 were obtained without repeatedly simulating the wave propagation. One can see in Fig. 8 a good matching between the observed and the computed marigrams in these sensors. As shown in [11], adding data recorded by the DART buoys 4-32411 and 5-43413 to the computational process did not improve the overall in-

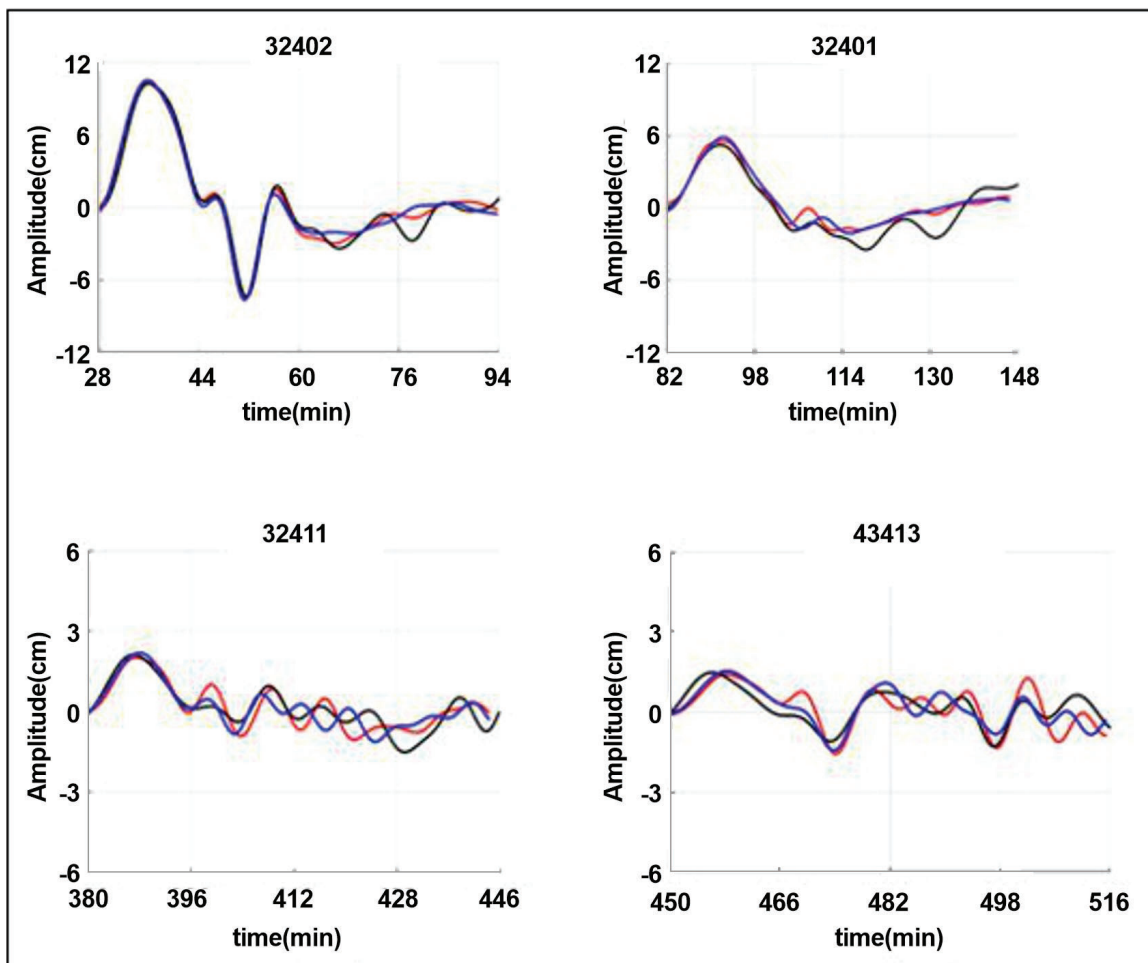


Fig. 8. Comparison of the amplitudes of the observed marigrams (the black lines) and computed ones from the data of DART buoys 1-32402, 2-32401, 3-32412 (the red lines) and data of DART buoys 1-32402 and 2-32401 (the blue lines); on the horizontal axes: time from the beginning of the event (in minutes).

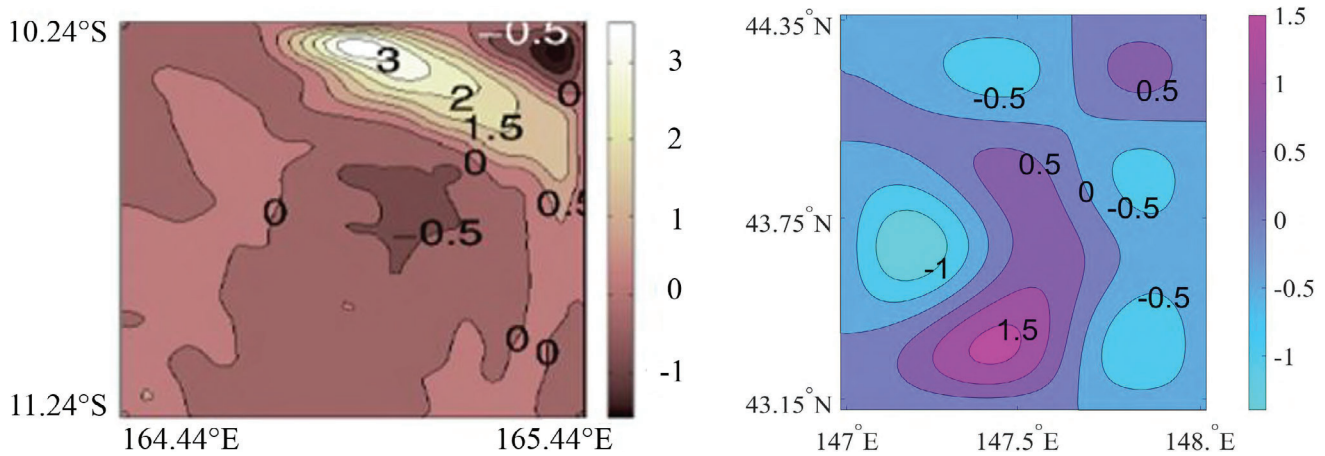


Fig. 9. The initial sea-surface displacements as inversion result based on the data recorded by the stations: (left) *Model 2*: using the DART buoys 1-55012 and 5-52406, $r = 21$; (right) *Model 3*: using the tide gauges 1-Kushiro, 2-Tokachikou, and 5-Miyako, $k_{mx} = 4$; $k_{ny} = 4$; $r = 12$. The sea surface displacement scaled in meters; the longitude and the latitude are along horizontal and vertical axes, respectively.

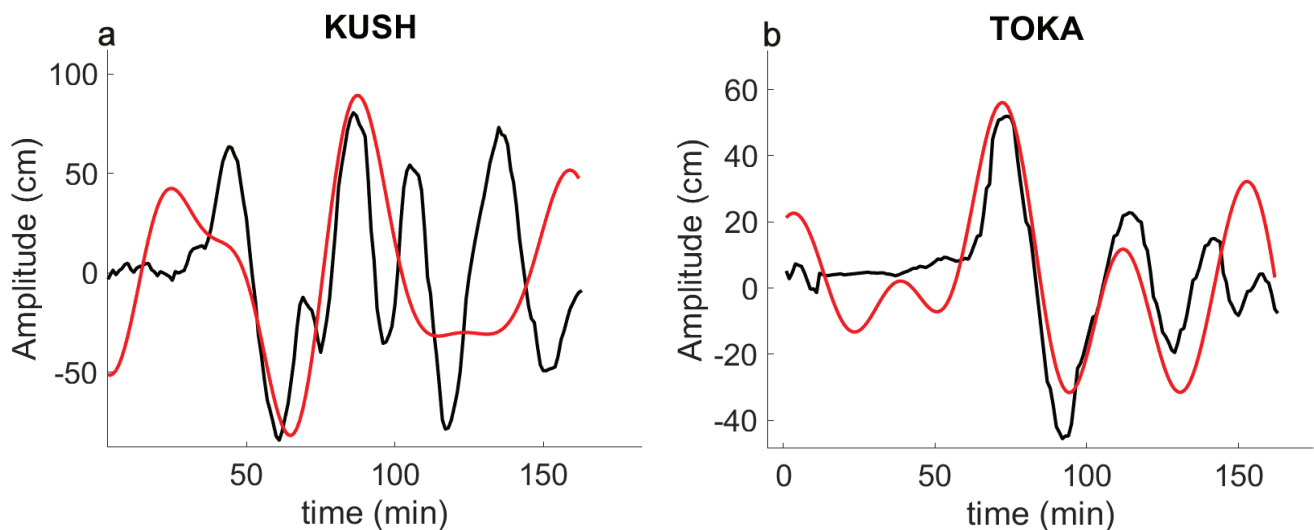


Fig. 10. Comparison of reconstructed (the red lines) and observed marigrams (the black lines) for sensors: (a) 1-Kushiro (has not been used for inversion); (b) 2-Tokachikou (has been used for inversion). Inversion was made with tide gauges data: 2-Tokachikou and 4-Hachinohe; $k_{mx} = 5$; $k_{ny} = 5$; $N_t = 162$ min.

version result that supports the idea of the “most informative” data.

Model 2. Data of DART buoys 1-55012 and 5-52406 were defined as the most informative. As shown in Fig. 6 b, the total specific energy in the locations of these buoys amounted to 74 % of the total energy. The result of the inversion with data generated by these DART buoys is represented in Fig. 9 a. It should be noted that this result will not change if one adds data from the other sensors of the observation system (see [12]).

Model 3. The result of recovering the tsunami source based on data recorded by tide gauges 1-Kushiro, 2-Tokachikou and 5-Miyako is shown

in Fig. 9 b. As follows from Fig. 6 c, using records of Miyako sensor has little effect in the inversion result.

Analyzing the amplitudes of modes in Fig. 3 c, we applied the above methodology to the *Model 3*. The data recorded by the tide gauge 2-Tokachikou should to be define as the most informative. The last is apparently caused by the direction of the source radiation and the nature of the bathymetry of the western slope of the Kuril-Kamchatka Trench. The diagram in Fig. 6 c shows that the data from tide gauges 2-Tokachikou together with 4-Hachinohe, or the data from 2-Tokachikou together with 1-Kushiro accumulate about

2/3 of the specific energy. Thus, the first of the above-mentioned observation systems makes it possible to reconstruct the wave amplitudes at the “point of interest” that it is the Kushiro sensor location, in this case.

The reconstructed marigrams obtained at the locations: 2-Tokachikou (has been used for inversion) and 1-Kushiro (has not been used for inversion), are presented in Figures 10 a and 10 b in comparison with the observed ones.

Conclusion

In order to improve the result of tsunami source inversion based on truncated singular value decomposition method, we proposed a technique for a reasonable choice of the key inversion parameters: the value of r , the number of the spatial harmonics and the most informative observation sensors. The approach based on the distribution of the specific energy of the tsunami wave across the locations of the sensors has shown its efficiency in choosing the most informative data for the recovering a tsunami source. We tested the fast-run algorithm for selecting an optimal tsunami observation dataset against three real-life tsunami events: the Chilean Illapel tsunami on September 16, 2015, the tsunami near the Solomon Islands on February 6, 2013, and the Shikotan tsunami on October 4, 1994. This algorithm is of particular importance in the development of future tsunami warning systems.

The proposed methodology is the following. First, the tsunamigenic zone is covered by a set of target domains. For each of them, the direct problems of wave propagation from the model sources (set of spatial harmonics) are solved. Numerical simulation propagates the model sources up to all sensors of the observation system, including both real-life stations and “fictitious” ones (locations without observations, but with an option for quick calculation of the wave amplitudes). The result of this step is the matrix of key system for each target domain. Second, the dimension of the solution subspace and the associated optimal number of spatial harmonics are determined. Third, an analysis of the distribution of the specific energy

of the wave across the locations of real-life sensors is carried out for each model source. Energy distribution is taken as a basis for selecting the set of the most informative sensors. Finally, the sensor locations defined as the most informative ones for multiple target domains should be considered as top candidates for creating an optimal observation system.

We have demonstrated that the use of the proposed algorithms to determine the key parameters makes it possible to obtain the inversion result with sufficient reliability. Moreover, within the r-resolution method it is possible to obtain rapidly the wave amplitudes at the locations of “fictitious” sensors without solving the direct problem again. The last feature of this approach makes it suitable for real-time tsunami warning.

References

1. Rabinovich A.B., Eblé M.C. **2015**. Deep-ocean measurements of tsunami waves. *Pure and Applied Geophysics*, 172(12): 3281–3312. <https://doi.org/10.1007/s00024-015-1058-1>
2. Omira R., Baptista M.A., Matias L., Miranda J.M., Catita C., Carrilho F., Toto E. **2009**. Design of a sea-level tsunami detection network for the Gulf of Cadiz. *Natural Hazards and Earth System Sciences*, 9: 1327–1338. <https://doi.org/10.5194/nhess-9-1327-2009>
3. Spillane M.C., Gica E., Titov V.V., Mofjeld H.O. **2008**. Tsunameter network design for the US DART arrays in the Pacific and Atlantic Oceans. *NOAA Technical Memorandum OAR PMEL*, 143 (165 p.).
4. Mulia I.E., Gusman A.R., Satake K. **2017**. Optimal design for placements of tsunami observing systems to accurately characterize the inducing earthquake. *Geophysical Research Letters*, 44. <https://doi.org/10.1002/2017gl075791>
5. Mulia I.E., Satake K. **2021**. Synthetic analysis of the efficacy of the S-net system in tsunami forecasting. *Earth, Planets and Space*, 73(1): 36. <https://doi.org/10.1186/s40623-021-01368-6>
6. Voronina T.A., Romanenko A.A. **2016**. The new method of tsunami source reconstruction with r-resolution inversion method. *Pure and Applied Geophysics*, 173(12): 4089–4099. <https://doi.org/10.1007/s00024-016-1286-z>
7. Voronina T.A. **2016**. Recovering a tsunami source and designing an observational system based on an r-resolution method. *Numerical Analysis and Applications*, 9(4): 267–276. <https://doi.org/10.1134/S1995423916040017>

8. Voronin V.V., Voronina T.A., Tcheverda V.A. **2015**. Inversion method for initial tsunami waveform reconstruction. *Natural Hazards and Earth System Sciences*, 15: 1251–1263. <https://doi.org/10.5194/nhess-15-1251-2015>
9. Percival D.B., Denbo D.W., Eble M.C., Gica E., Mofjeld H.O., Spillane M.C., Tang L., Titov V. **2011**. Extraction of tsunami source coefficients via inversion of DART buoy data. *Natural Hazards*, 58: 567–590.
10. Ivetskaya T.N., Shevchenko G.V. **1997**. Spectral analysis for Shikotan tsunami records (October 5, 1994). In: *Manifestations of certain tsunami. 1993 and 1994 Tsunami on the Russian coast*. Yuzhno-Sakhalinsk: IMGG FEB RAS, p. 105–118. (In Russ.).
11. Voronina T.A., Voronin V.V. **2021**. A study of implementation features of the r-solution method for tsunami source recovery in the case of the Illapel Tsunami 2015. *Pure and Applied Geophysics*, 178: 4853–4863. doi:10.1007/s00024-021-02843-7
12. Voronina T.A., Voronin V.V. **2022**. Selecting the most informative set of the deep-ocean tsunami sensors based on the r-solution method. *Numerical Methods and Programming*, 23: 230–239. (In Russ.). doi:10.26089/NumMet.v23r314
13. Satake K., Heidarzadeh M.A. **2017**. Review of source models of the 2015 Illapel, Chile earthquake and insights from tsunami data. *Pure Applied Geophysics*, 174: 1–9. doi:10.1007/s00024-016-1450-5

About the Authors

Voronina, Tatyana A. (<https://orcid.org/0000-0002-3566-6203>), Candidate of Sciences (Physics and Mathematics), Senior Researcher, Tsunami Laboratory, Institute of Computational Mathematics and Mathematical Geophysics of the Siberian Branch of RAS, Novosibirsk, tanvor@bk.ru

Voronin, Vladislav V. (<https://orcid.org/0000-0002-1727-1873>), Candidate of Sciences (Physics and Mathematics), Associate Professor, Higher Mathematics Chair, Department of mathematics and mechanics, Novosibirsk State University, Novosibirsk, vladvor48@bk.ru

Об авторах

Воронина Татьяна Александровна (<https://orcid.org/0000-0002-3566-6203>), кандидат физико-математических наук, старший научный сотрудник лаборатории математического моделирования волн цунами, Институт вычислительной математики и математической геофизики СО РАН, Новосибирск, tanvor@bk.ru

Воронин Владислав Владимирович (<https://orcid.org/0000-0002-1727-1873>), кандидат физико-математических наук, доцент кафедры высшей математики ММФ, Новосибирский государственный университет, Новосибирск, vladvor48@bk.ru

Поступила 20.08.2023
Принята к публикации 11.09.2023

Received 20 August 2023
Accepted 11 September 2023